Development of Triantennary N-Acetylgalactosamine Conjugates as Degraders for Extracellular Proteins

Yaxian Zhou,[1] Peng Teng,[1] and Weiping Tang[1,2*]

[1.] School of Pharmacy, University of Wisconsin-Madison, Madison, WI, USA 56305.

[2.] Department of Chemistry, University of Wisconsin-Madison, Madison, WI, USA 56306.

[*]All correspondence should be addressed to weiping.tang@wisc.edu

Abstract

Targeted protein degradation (TPD) technology has drawn significant attention from researchers in both academia and industry. It is rapidly evolved as a new therapeutic modality and also a useful chemical tool in selectively depleting various protein targets. As most efforts focus on cytosolic proteins using PROteolysis TArgeting Chimera (PROTAC), LYsosome TArgeting Chimera (LYTAC) recently emerged as a promising technology to deliver extracellular protein targets to lysosome for degradation through cation-independent mannose-6-phosphate receptor (CI-M6PR). In this study, we exploited the potential of asialoglycoprotein receptor (ASGPR), a lysosomal targeting receptor specifically expressed on liver cells, for the degradation of extracellular proteins. The ligand of ASGPR, triantennary *N*-acetylgalactosamine (tri-GalNAc), was conjugated to biotin, antibodies, or fragments of antibodies to generate a new class of degraders. We demonstrated that the extracellular protein targets could be successfully internalized and delivered into lysosome for degradation in a liver cell line specifically by these degraders. We also observed that more efficient delivery could be achieved for smaller degrader/target complexes. This work will add a new dimension to the TPD with cell type specificity.

Introduction

Protein degradation is essential for maintaining cellular protein homeostasis. Most proteins in eukaryotic cells are degraded through ubiquitin-proteasome system, where the E3

ubiquitin ligase recognizes a specific protein substrate and tags multiple ubiquitin motifs to it, leading to the subsequent proteolysis by the proteasome[1, 2]. Lysosome is another major destination for protein degradation. Through autophagy and endocytosis, both intracellular and extracellular proteins enclosed in vesicles can be delivered into lysosomes for degradation[3, 4]. Based on these mechanisms, targeted protein degradation by chimeric molecules emerged as a novel therapeutic modality. These chimeras are heterobifunctional molecules with one end binding to the protein of interest (POI) and the other end directing the ternary complex towards a certain degradation pathway. PROteolysis TArgeting Chimera (PROTAC) has received the most attention to date. PROTACs contain an E3 ligase ligand to route the targeted protein to the proteasome for degradation[5, 6]. More recently, AUtophagy-TArgeting Chimera (AUTAC) was developed to degrade not only proteins but also organelles by using S-guanylation as the tag for autophagy[7]. However, these two types of chimeras are only capable of depleting cytoplasmic proteins or membrane proteins with a cytosolic binding domain. To broaden the scope of targets to include proteins without cytosolic binding domains, Bertozzi's group first developed LYsosome TArgeting Chimeras (LYTACs) by conjugating the ligand of the ubiquitously expressed cation-independent mannose-6-phosphate receptor (CI-M6PR) on the cell surface with a molecule that binds to the extracellular protein target[8]. The receptor-ligand interaction triggers the internalization of the extracellular proteins through receptor-mediated endocytosis, further inducing the degradation of the targets in the lysosome. CI-M6PR has been used to deliver therapeutic drugs conjugated with mannose-6-phosphate (M6P) derivatives for lysosomal enzyme replacement therapy and cancer treatment[9, 10]. Various molecules, such as peptides, proteins or liposome, were covalently linked to the modified M6P with enhanced affinity and stability to achieve targeted drug delivery[11-14]. To extend the usage of M6PR/M6P system to targeted protein degradation, LYTAC was constructed by conjugating a mixture of polyglycopeptides containing multiple M6P analogues to the antibody of POI. Different from drug delivery process, which involves the

internalization of a covalent linked M6P-protein target, LYTAC allows the trafficking of a complex formed by the non-covalent interaction between the protein target and LYTAC. It has been shown that LYTAC could successfully degrade both secreted and membrane proteins in the lysosome through CI-M6PR.[8]

Asialoglycoprotein receptor (ASGPR) is another well-defined lysosomal targeting receptor, responsible for clearing glycoproteins via clathrin-mediated endocytosis and lysosomal degradation. Unlike CI-M6PR, ASGPR is primarily and highly expressed in hepatocytes with 500,000 copies per cell[15]. The unique expression pattern together with rapid recycling rate (~15 min)[16] make ASGPR a promising candidate for liver-specific targeted protein degradation. It has been reported that ASGPR binds to galactose (Gal) and N-acetylgalactosamine (GalNAc), with a higher affinity to the latter than the former, in the presence of Ca^{2+} ions[17, 18]. Studies using both cluster galactosides and synthetic oligosaccharides indicated that trivalent GalNAc ligand with a 15-20 Å spacing between each sugar exhibited the highest binding affinity and efficiency for endocytosis compared to mono- and bivalent GalNAc ligands[19, 20]. Further research on triantennary ligand revealed that cargo size below 70 nm is also required for the proper receptor recognition and efficient endocytosis[21]. The comprehensive understanding of receptor-ligand interaction paved the way for the application of ASGRP/triantennary GalNAc (tri-GalNAc) system in targeted drug delivery, especially for oligonucleotide therapy. Many tri-GalNAc-modified therapeutic nucleic acid agents, including siRNAs, anti-miRNAs and antisense oligonucleotides (ASOs), are now in preclinical or clinical studies[22, 23]. It has been shown that the conjugation of tri-GalNAc facilitates the uptake of the oligonucleotides and thus much lower dose is required compared to the free version[24, 25]. Besides direct labeling of the therapeutic drugs, tri-GalNAc was also tagged to some drug carriers, such as lipid nanoparticle or poly-(amidoamine) (PAMAM) dendrimer to achieve targeted delivery[26, 27]. It was reported that modifying poly-c-glutamic acids (PGA) with tri-GalNAc resulted in

the exclusive distribution in mice liver, while the non-modified PGA were excreted into urine[28]. However, despite the extensive use in drug delivery, the possibility of ASGPR-mediated targeted protein degradation hasn't been exploited prior to our study. During the preparation of this manuscript, research groups of Spiegel and Bertozzi independently reported their elegant design of chimeric molecules with tri-GalNAc for targeted protein degradation in liver cells[29, 30]. While the former focused on small molecule-based lysosome targeting degraders[29], the latter investigated antibody-based degraders for extracellular protein targets[30]. Inspired by Bertozzi's pioneering work on LYTACs based on CI-M6PR and due to our interest in both targeted protein degradation[31-34] and carbohydrate chemistry[35, 36], we initiated the investigation of ASGPR-mediated targeted protein degradation using chimeric molecules bearing a trivalent GalNAc ligand as liver cell-specific degraders for extracellular proteins (Fig. 1). Since liver is the major place for protein catabolism, selectively delivering undesired proteins to liver should be advantageous over ubiquitously delivery of the protein targets to various types of cells for many therapeutic applications.

Results and Discussion

Tri-GalNAc-biotin conjugate 1, a small molecule lysosome targeting degrader, can facilitate the uptake of NeutrAvidin through ASGPR in HepG2 cells.

As our initial study, we employed NeutrAvidin (NA) as the targeted protein. Commercially available tri-GalNAc-biotin conjugate **1** was used as the ligand of ASGPR to examine the uptake of NA (Fig. 2A). HepG2 cells were treated with 2 μM of **1** and 500 nM of fluorescently labeled NA-650 concurrently for 4 h, and the fluorescent intensity inside the cells was measured by the plate reader to indicate the uptake of the NA-650. Our data showed that NA-650 was internalized into the cell in a time-dependent manner in the presence of **1**. No increase of the fluorescent signal was observed when the cells were treated with NA-650 alone or in the presence of negative control, tri-GalNAc-COOH **2**

(Fig. 2B). The treatment of increasing concentration of **1** showed reduced uptake of NA-650 at high doses, suggesting that the formation of binary complex between **1** and receptor becomes dominant over the formation of ternary complex NA-650/**1**/receptor with excess degrader **1** (Fig. S1A), which is often termed as hook effect[37]. We next extended the incubation time for **1** and NA-650 in HepG2 cells to 24 h. A continuous increase of the fluorescent signal was detected in the early phase while the signal gradually reached the plateau after 16-20 h (Fig. S1B).

To verify that the internalization of NA-650 was mediated through ASGPR, various concentrations of **2** were added to compete for the receptor with the **1**/NA-650 complex. The results showed that the uptake of NA-650 negatively correlated with the amount of **2**, suggesting that the internalization of NA-650 required the interaction between **1**/NA-650 complex and ASGPR (Fig. 2C). Moreover, significant lower uptake of NA-650 in A549 cells, which lack the expression of ASGPR compared to HepG2 cells, further confirmed the involvement of ASGPR in the transportation of NA-650 and indicated that the biotinylated ligand containing tri-GalNAc specifically delivered the targeted protein into liver cells (Fig. 2D). Similar to Fig. 2B, compound **2** without the biotin moiety failed to deliver NA-650 to HepG2 or A549 cells.

Tri-GalNAc-biotin conjugate 1 delivers NeutrAvidin to lysosome for degradation

Next, we investigated whether NA-650 was delivered into lysosomes and degraded after being endocytosed into the cell. Confocal images showed the distribution of NA-650 in the cytoplasm and co-localization with the lysosome indicated by Lysotracker. This confirmed the ASGPR-mediated uptake and trafficking of the protein target to the lysosome (Fig. 3A). To evaluate the degradation of NA-650, HepG2 cells were incubated with NA-650 and **1** for 1 h, followed by the replacement of fresh media to allow further degradation. Compared to the amount of NA-650 enriched in the cell within 1 h incubation, decreasing amounts of

NA-650 were detected at 3 h, 6 h, 24 h post media change. The addition of protease inhibitor leupeptin moderately arrested the degradation of NA-650 at each time point (Fig. 3B). These data indicated that the degradation of NA-650 occurred after it was transported into the lysosome.

A tri-GalNAc labelled full length antibody (goat anti-mouse IgG) facilitates the uptake of its protein target (mouse anti-biotin IgG-647) with a relatively low efficiency. Given the successful internalization and degradation of NA by **1** in the model system, we hypothesized that an antibody conjugated with tri-GalNAc can function similarly as **1** tested above - capturing the extracellular targeted protein and delivering it into the lysosome for degradation. To validate the feasibility of our hypothesis, we first functionalized an antibody with tri-GalNAc to generate an antibody-based degrader (tri-GalNAc-antibody). Tri-GalNAc-COOH **2** was converted to its active *N*-hydroxysuccinimide (NHS)-ester **3** under standard conditions. The antibody was then conjugated with NHS ester **3** by reacting with the lysine residues on the antibody. After testing different molar ratios for the antibody conjugation, we found that the best labeling efficiency was achieved by using 25 equivalent of NHS ester **3** (Fig. 4A). Moreover, comparing the internalization of antibodies coupled with various equivalents of tri-GalNAc revealed that higher degree of tri-GalNAc labeling on the antibody resulted in a greater internalization capacity (Fig. S2).

We then examined the uptake of the targeted protein by co-treating HepG2 cells with tri-GalNAc-modified goat anti-mouse IgG (Ab-GN) and fluorescent protein target mouse anti-biotin IgG-647 for 6 h. The addition of Ab-GN increased the uptake of mouse anti-biotin IgG-647 compared to the cells treated with mouse anti-biotin IgG-647 alone, but the efficiency was relatively low (Fig. 4B). To identify the factors that gave rise to the low uptake efficiency, fluorescent goat anti-mouse IgG-647 was directly labeled with NHS

ester **3** (Ab-647-GN). Greater fluorescent intensity was observed in the cells treated with Ab-647-GN alone than the cells co-treated with Ab-GN and mouse IgG-647 (Fig. 4C), suggesting the low uptake of the targeted protein was not restrained by the internalization efficiency of tri-GalNAc-Ab itself. We then pre-incubated mouse anti-biotin IgG-647 and Ab-GN to allow the complex formed prior to the treatment. The pre-mixing did not enhance the amount of internalized mouse IgG-647 (Fig. 4C), suggesting that the complex formation is not the rate-limiting step for the tri-GalNAc-Ab mediated uptake.

Comparison of the uptake efficiency of the protein targets (mouse anti-biotin IgG-647 and mouse anti-rabbit IgG-647) mediated by tri-GalNAc labelled full length antibody, Fab dimer, and Fab.

It has been reported that the size of the complex plays a critical role in the recognition and processing by the ASGPR. Efficient uptake of liposome could only be achieved when their sizes are less than 70 nm[21]. To compare the internalization efficiency of the protein target by degraders with different sizes, we labelled goat anti-mouse IgG Fab dimer (MW = 110 kDa) and Fab monomer (MW = 50 kDa) with NHS ester **3** to yield two smaller degraders, F(ab')2-GN and Fab-GN (Fig. 5A). The MW of the parent full size antibody goat anti-mouse IgG is 150 kDa. All three antibodies (full length goat anti-mouse IgG, Fab dimer, and Fab) should bind to mouse anti-biotin IgG-647 with similar affinity. We then co-treated HepG2 cells with 50 nM of the protein target (mouse anti-biotin IgG-647) together with 25 nM of goat anti-mouse IgG (Ab), goat anti-mouse IgG F(ab')2-647 (abbreviated as F(ab')2-647) and goat anti-mouse IgG Fab (Fab) with or without tri-GalNAc (GN) labeling. The amount of florescent mouse anti-biotin IgG-647 inside the cells was monitored 6 h post-treatment. In gel fluorescence analysis showed that all three types of tri-GalNAc-antibodies were able to enhance the internalization of mouse anti-biotin IgG-647 compared to the cells with only mouse anti-biotin IgG-647 treatment. Among them, F(ab')2-647-GN exhibited similar uptake efficiency as Ab-GN, while Fab-GN significantly boosted the

uptake of the mouse IgG-647 (Fig. 5B). No increased uptake of the protein target was observed when the cells were treated with antibodies without GalNAc labeling and the protein target compared with treating the cells with protein target alone (Fig. 5B). No obvious signal was observed when the cells were treated with tri-GalNAc-antibodies alone (Fig. 5B). We then decided to confirm this trend by studying three tri-GalNAc-Antibody-mediated uptake of another protein target, fluorescent mouse anti-rabbit IgG-647. Our results again showed that the highest target uptake was achieved by Fab-GN (Fig. S3). Fab-GN, the tri-GalNAc conjugate with the lowest molecular weight and size, can promote the most efficient uptake of two different protein targets among the three antibody-based degraders, suggesting that the size of the tri-GalNAc-Ab may affect the endocytosis process mediated by ASGPR.

Next, we confirmed the uptake of protein target was dependent on the interaction between tri-GalNAc and ASGPR, which is mainly expressed in liver cells, by incubating the Fab-GN and mouse anti-biotin IgG-647 with HepG2 cells and A549 cells respectively. The amount of mouse IgG-647 was significantly higher in the Fab-GN treated HepG2 cells than the other groups, suggesting the protein target can only be efficiently transported into ASGPR-expressing cell with the assistance of tri-GalNAc-modified antibody (Fig. 5C). The degradation of internalized mouse IgG-647 was detected after the removal of Fab-GN and mouse IgG-647 from the media for 3 h. Leupeptin moderately inhibited the degradation, indicating that the protein was depleted through lysosome degradation pathway (Fig. 5D).

Comparison of the uptake efficiency of proteins with different sizes mediated by tri-GalNAc-biotin conjugate 1.

Different uptake efficiencies were observed for two different protein targets (mouse anti-biotin IgG-647 and mouse anti-rabbit IgG-647) using three different antibody-based degraders: tri-GalNAc labelled full size antibody, Fab dimer, and Fab. We next decided to

compare the uptake efficiency of proteins in different sizes using the same small molecule-based degrader, **1**. In addition to NA with a MW of 60 kDa and K_d of ~10^{-15} M with biotin, mouse anti-biotin-647 with a MW of 150 kDa can also bind to biotin with high affinity (K_d = ~10^{-10} M)[38]. Incubating mouse anti-biotin IgG-647 with goat anti-mouse IgG or anti-mouse IgG Fab fragment could enable the formation of protein complexes with increased molecular weight and sizes. HepG2 cells were treated with NA-650 (P1), mouse anti-biotin IgG-647 (P2), pre-mixed mouse anti-biotin IgG-647/goat anti-mouse IgG Fab (P3) and pre-mixed mouse anti-biotin IgG-647/goat anti-mouse IgG (P4) in the presence of **2** or **1** for 6 h. The results showed that the uptake efficiency of protein targets decreased as the size of the complex increased when cells co-treated with same amount of **1** (Fig. 6). Acid **2** didn't induce the internalization of protein targets at all. Consistent with the results of tri-GalNAc-antibodies, **1** also displayed a higher uptake efficiency for the smaller degrader-target complex. The exceptionally high uptake efficiency of NA is likely due to the high affinity between NA and biotin (K_d = 10^{-15} M) and multiple biotin binding sites on NA[38, 39]. The affinity of **1** to mouse anti-biotin IgG-647 (P2), pre-mixed mouse anti-biotin IgG-647/goat anti-mouse IgG Fab (P3), and pre-mixed mouse anti-biotin IgG-647/goat anti-mouse IgG (P4) should be very similar. The most reasonable explanation of the decreased uptake efficiency from P2 to P3 and from P3 to P4 appears to be the increased size of the target complexes. Our data again indicate that the internalization driven by a small molecule tri-GalNAc-conjugate through ASGPR is more efficient for smaller degrader-protein target complexes.

Conclusion

The emergence of chimeric molecules that are capable of depleting pathogenic proteins through native degradation pathways have the potential to overcome a major limitation of traditional therapeutic strategies, which generally need to bind to the protein target and alter its function. Targeted protein degradation using chimeric molecules only needs a

binder to the protein target. Depletion of the entire pathogenic protein also offers unique advantages over functional inhibition in many cases. However, the most developed targeted protein degradation strategy, namely PROTAC, is restricted to degrading intracellular targets. The M6P analogue-based LYTAC opened up a new direction of research area for targeted protein degradation by expanding the scope of targets to extracellular proteins. Similar to proteasome targeting degraders, where only handful of E3 ubiquitin ligase ligands are available, more lysosome targeting ligands need to be explored for expanded utilities of lysosome targeting degraders. We described our initial proof-of-concept studies using a tri-GalNAc-biotin small molecule and tri-GalNAc labelled antibodies to deliver the extracellular protein targets into the lysosome for degradation. We have shown that the internalization and lysosomal degradation of the protein targets through ASGPR are possible by both small molecule-based and antibody-based lysosome targeting degraders. We also observed that smaller complexes exhibited higher uptake efficiency in several cases. In addition to the well-known factors, such as the length of linker, the type of linker, polyvalency, binding affinities to the receptor and protein target, expression levels of receptor and protein target, the size of the complex may be an additional parameter for the optimization of triantennary GalNAc conjugate-mediated lysosomal degradation of extracellular proteins. Overall, our studies demonstrated the feasibility of ASGPR-mediated liver cell-specific targeted protein degradation strategy and uncovered a potential new therapeutic application of triantennary GalNAc in addition to its well-known utilities in liver-specific delivery of oligonucleotides.

Materials and Methods

General chemistry methods

Tri-GalNAc-biotin **1** and tri-GalNAc-COOH **2** were purchased from Sussex Research Laboratories Inc. Other reagents and solvents were purchased from Fisher Scientific and used as received. Tri-GalNAc-NHS ester **3** was prepared from tri-GalNAc-COOH **2** in the

presence of *N*-hydroxysuccinimide and N, N′ -dicyclohexylcarbodiimide in dimethylformamide (DMF) as used without further purification. The reaction was monitored by Agilent single quadrupole (SQ) LC/MS.

Cell culture

HepG2 cells were cultured in T75 flasks and maintained in low-glucose DMEM supplemented with 10% fetal bovine serum, 1% non essential amino acids, 1% sodium pyruvate, 1% L-glutamine and 1% penicillin/streptomycin under 5 % CO_2 at 37 °C. A549 cells were culture in T75 flasks and maintained in RPMI supplemented with 10% fetal bovine serum, 1% sodium pyruvate, 1% HEPES and 1% penicillin/streptomycin under 5 % CO_2 at 37 °C.

NeutraAvidin uptake experiments

Cells were seeded at 45,000 cells per well in 100 μL complete culture media in 96-well cell culture plates. The next day, the medium was replaced followed by the sequential addition of NeutrAvidin (NA)-650 alone or NA-650 and tri-GalNAc-biotin **1** or tri-GalNAc-COOH **2** with various concentrations. The cells were incubated at 37 °C for different time periods and then washed twice with PBS to removed extracellular NA-650. The uptake was determined by measuring the fluorescent intensity at 650 nm excitation/680 nm emission using the Synergy H1 microplate reader. Data was acquired using Gen5 software.

Competition assay

HepG2 cells were plated and treated with 500 nM of NA-650 and 2 μM of tri-GalNAc-biotin **1** in the same manner as mentioned above. Extra tri-GalNAc-COOH **2** (1, 2, 5, 10, 20 μM) was added at the same time before incubation. After 4 h, cells were washed twice with PBS, and the uptake of NA-650 was read by the plate reader as mentioned above.

Confocal microscopy

HepG2 cells were seeded onto 8-well chamber slides at the density of 20,000 cells/well in 200 μL of complete culture medium. After adhesion, cells were treated with 500 nM of NA-650 and 2 μM of tri-GalNAc-biotin **1** for 18 h at 37 °C, followed by the 30-min incubation with LysoTracker Green DND26 (100 nM) at 37 °C. Hoechst 33342 (5 ug/ml) was added 10 min before the end of incubation. After three washes with PBS, the live cells were imaged using FluoView confocal microscope at 20x magnification with a 10x eyepiece. All images were acquired by FV10-ASW and analyzed by ImageJ.

NeutraAvidin degradation analysis

HepG2 cells were seed at 250,000 cells per well in a 24-well plate. Next day, cells were incubated with 500 nM of NA-650 and 2 μM of tri-GalNAc-biotin **1** for 1 h followed by three washes with PBS. Cells were maintained subsequently in fresh media with or without 0.1 mg/mL leupeptin for another 3 h, 6 h, and 24 h before harvested for in gel fluorescence analysis.

Antibody labeling

The antibody solution was first loaded onto Zeba™ Spin Desalting Columns (7K MWCO, 0.5 ml) to remove the sodium azide before labeling. To label the antibody with tri-GalNAc, 50 μL of the secondary antibody (concentration above 1 mg/mL) in PBS was mixed with tri-GalNAc-NHS ester **3** at 1:3, 1:12 or 1:25 molar ratio. The reaction was incubated overnight at room temperature on a rotator, followed by filtration with 500 μL of PBS for 5 times using 10 kDa Amicon Centrifugal Filter.

Tri-GalNAc-antibody uptake experiment

HepG2 cells were plated at 45,000 cells per well in 100 μL complete culture media in a 96-well cell culture plate 8 h prior to the treatment. Cells were then incubated with 25 nM Ab-

647-GN with different modification levels for 16 h before measuring the fluorescence intensity in the cells.

Mouse IgG uptake experiment

HepG2 cells and A549 cells were plated at 250,000 cells per well in a 24-well plate. Complete growth media supplemented with 50 nM of mouse anti-biotin-IgG-647 (protein target in Fig. 5B) or mouse anti-rabbit-IgG-647 (protein target in Fig. S3) and 25 nM of tri-GalNAc labelled goat anti-mouse IgG, goat-anti-mouse IgG F(ab')2, or goat-anti-mouse IgG Fab was sequentially added. The cells were incubated at 37 °C for 6 h and then lysed for in gel fluorescence analysis.

Mouse IgG degradation analysis

HepG2 cells were seed at 250,000 cells per well in a 24-well plate. Next day, cells were incubated with 50 nM of mouse anti-biotin IgG-647 and 25 nM of tri-GalNAc goat-anti-mouse IgG Fab for 3 h followed by three washes with PBS. Cells were maintained subsequently in fresh media with or without 0.1 mg/mL leupeptin for another 3 h before harvested for in gel fluorescence analysis.

NeutrAvidin and IgG complex uptake experiment

HepG2 cells were plated at 250,000 cells per well in a 24-well plate. Next day, 50 nM mouse anti-biotin IgG-647 was mixed with 200 nM goat anti-mouse IgG or goat anti-mouse IgG Fab on a rotator at room temperature for 1 h before treatment. Cells were then respectively incubated with 50 nM NA-650, mouse anti-biotin IgG-647, anti-biotin IgG-647/goat anti-mouse IgG Fab and anti-biotin IgG-647/goat anti-mouse IgG complex together with 200 nM tri-GalNAc-COOH **2** or tri-GalNAc-biotin **1** for 6 h. The cells were then harvested and lysed for in gel fluorescence analysis.

Sources of key reagents and antibodies

Reagents and antibodies	Vendor	Catalog #
Trivalent GalNAc-biotin **1**	Sussex Research	BT000130
Trivalent GalNAc-COOH **2**	Sussex Research	PE000130
NeutrAvidin protein, DyLight 650	Fisher Scientific	84607
LysoTracker Green DND26	Fisher Scientific	L7526
Hoechst 33342	Fisher Scientific	H3570
Leupeptin	Sigma-Aldrich	L2884-5MG
AffiniPure Goat Anti-Mouse IgG	Jackson ImmunoResearch	115-005-062
Goat anti-mouse IgG, Alexa Fluor®647	Invitrogen	A-21235
F(ab')2-Goat anti-mouse IgG, Alexa Fluor®647	Invitrogen	A-21237
Affinipure Fab Fragment Goat anti-mouse IgG	Jackson ImmunoResearch	115-007-003
Anti-Biotin Mouse Monoclonal Antibody (Alexa Fluor®647)	Jackson ImmunoResearch	200-602-211
Mouse Anti-Rabbit IgG Antibody (Alexa Fluor® 647)	Jackson ImmunoResearch	211-605-109

Funding
We thank the University of Wisconsin-Madison for financial support.

Author contributions
Y.Z. and W.T. conceived the project. Y.Z. carried out all biological experiments and interpreted the data. P.T. prepared compound **3** from **2** and provided insights to the project. Y.Z. and W.T. wrote the manuscript with input from all authors.

Competing interests

The authors have no relevant financial interest to declare.

References

1. Rock, K. L.; Gramm, C.; Rothstein, L.; Clark, K.; Stein, R.; Dick, L.; Hwang,

D.; Goldberg, A. L., Inhibitors of the proteasome block the degradation of most cell proteins and the generation of peptides presented on MHC class I molecules. *Cell* **1994,** *78* (5), 761-71.
2. Ciechanover, A.; Schwartz, A. L., The ubiquitin-proteasome pathway: the complexity and myriad functions of proteins death. *Proc Natl Acad Sci U S A* **1998,** *95* (6), 2727-30.
3. Yim, W. W.; Mizushima, N., Lysosome biology in autophagy. *Cell Discov* **2020,** *6*, 6.
4. Lamb, C. A.; Dooley, H. C.; Tooze, S. A., Endocytosis and autophagy: Shared machinery for degradation. *Bioessays* **2013,** *35* (1), 34-45.
5. Sakamoto, K. M.; Kim, K. B.; Kumagai, A.; Mercurio, F.; Crews, C. M.; Deshaies, R. J., Protacs: chimeric molecules that target proteins to the Skp1-Cullin-F box complex for ubiquitination and degradation. *Proc Natl Acad Sci U S A* **2001,** *98* (15), 8554-9.
6. Schapira, M.; Calabrese, M. F.; Bullock, A. N.; Crews, C. M., Targeted protein degradation: expanding the toolbox. *Nat Rev Drug Discov* **2019,** *18* (12), 949-963.
7. Takahashi, D.; Moriyama, J.; Nakamura, T.; Miki, E.; Takahashi, E.; Sato, A.; Akaike, T.; Itto-Nakama, K.; Arimoto, H., AUTACs: Cargo-Specific Degraders Using Selective Autophagy. *Mol Cell* **2019,** *76* (5), 797-810.e10.
8. Banik, S. M.; Pedram, K.; Wisnovsky, S.; Ahn, G.; Riley, N. M.; Bertozzi, C. R., Lysosome-targeting chimaeras for degradation of extracellular proteins. *Nature* **2020,** *584*, 291-297.
9. Basile, I.; Da Silva, A.; El Cheikh, K.; Godefroy, A.; Daurat, M.; Harmois, A.; Perez, M.; Caillaud, C.; Charbonné, H. V.; Pau, B.; Gary-Bobo, M.; Morère, A.; Garcia, M.; Maynadier, M., Efficient therapy for refractory Pompe disease by mannose 6-phosphate analogue grafting on acid α-glucosidase. *J Control Release* **2018,** *269*, 15-23.
10. Bouffard, E.; Mauriello Jimenez, C.; El Cheikh, K.; Maynadier, M.; Basile, I.; Raehm, L.; Nguyen, C.; Gary-Bobo, M.; Garcia, M.; Durand, J. O.; Morère, A., Efficient Photodynamic Therapy of Prostate Cancer Cells through an Improved Targeting of the Cation-Independent Mannose 6-Phosphate Receptor. *Int J Mol Sci* **2019,** *20* (11), 2809.
11. Hyun, J. Y.; Kim, S.; Lee, H. S.; Shin, I., A Glycoengineered Enzyme with Multiple Mannose-6-Phosphates Is Internalized into Diseased Cells to Restore Its Activity in Lysosomes. *Cell Chem Biol* **2018,** *25* (10), 1255-1267.e8.
12. Das, S.; Parekh, N.; Mondal, B.; Gupta, S., Controlled Synthesis of End-Functionalized Mannose-6-phosphate Glycopolypeptides for Lysosome Targeting. *ACS Macro Lett.* **2016,** *5*, 809-813.
13. Crucianelli, E.; Bruni, P.; Frontini, A.; Massaccesi, L.; Pisani, M.; Smorlesi, A.; Mobbili, G., Liposomes containing mannose-6-phosphate-cholesteryl conjugates for lysosome-specific delivery. *RSC Advances* **2014,** *4* (102), 58204-58207.
14. Agarwal, V.; Toshniwal, P.; Smith, N. E.; Smith, N. M.; Li, B.; Clemons, T. D.;

Byrne, L. T.; Kakulas, F.; Wood, F. M.; Fear, M.; Corry, B.; Swaminathan Iyer, K., Enhancing the efficacy of cation-independent mannose 6-phosphate receptor inhibitors by intracellular delivery. *Chem Commun (Camb)* **2016,** *52* (2), 327-30.
15. Spiess, M., The asialoglycoprotein receptor: a model for endocytic transport receptors. *Biochemistry* **1990,** *29* (43), 10009-18.
16. Schwartz, A. L.; Fridovich, S. E.; Lodish, H. F., Kinetics of internalization and recycling of the asialoglycoprotein receptor in a hepatoma cell line. *J Biol Chem* **1982,** *257* (8), 4230-7.
17. Baenziger, J. U.; Fiete, D., Galactose and N-acetylgalactosamine-specific endocytosis of glycopeptides by isolated rat hepatocytes. *Cell* **1980,** *22* (2 Pt 2), 611-20.
18. Drickamer, K., Ca2+-dependent carbohydrate-recognition domains in animal proteins. *Curr Opin Struct Biol.* **1993,** *3* (3), 393-400.
19. Lee, Y. C.; Townsend, R. R.; Hardy, M. R.; Lönngren, J.; Arnarp, J.; Haraldsson, M.; Lönn, H., Binding of synthetic oligosaccharides to the hepatic Gal/GalNAc lectin. Dependence on fine structural features. *J Biol Chem* **1983,** *258* (1), 199-202.
20. Biessen, E. A.; Beuting, D. M.; Roelen, H. C.; van de Marel, G. A.; van Boom, J. H.; van Berkel, T. J., Synthesis of cluster galactosides with high affinity for the hepatic asialoglycoprotein receptor. *J Med Chem* **1995,** *38* (9), 1538-46.
21. Rensen, P. C.; Sliedregt, L. A.; Ferns, M.; Kieviet, E.; van Rossenberg, S. M.; van Leeuwen, S. H.; van Berkel, T. J.; Biessen, E. A., Determination of the upper size limit for uptake and processing of ligands by the asialoglycoprotein receptor on hepatocytes in vitro and in vivo. *J Biol Chem* **2001,** *276* (40), 37577-84.
22. Glazier, D. A.; Liao, J.; Roberts, B. L.; Li, X.; Yang, K.; Stevens, C. M.; Tang, W., Chemical Synthesis and Biological Application of Modified Oligonucleotides. *Bioconjug Chem* **2020,** *31* (5), 1213-1233.
23. Huang, Y., Preclinical and Clinical Advances of GalNAc-Decorated Nucleic Acid Therapeutics. *Mol Ther Nucleic Acids* **2017,** *6*, 116-132.
24. Prakash, T. P.; Graham, M. J.; Yu, J.; Carty, R.; Low, A.; Chappell, A.; Schmidt, K.; Zhao, C.; Aghajan, M.; Murray, H. F.; Riney, S.; Booten, S. L.; Murray, S. F.; Gaus, H.; Crosby, J.; Lima, W. F.; Guo, S.; Monia, B. P.; Swayze, E. E.; Seth, P. P., Targeted delivery of antisense oligonucleotides to hepatocytes using triantennary N-acetyl galactosamine improves potency 10-fold in mice. *Nucleic Acids Res* **2014,** *42* (13), 8796-807.
25. Schmidt, K.; Prakash, T. P.; Donner, A. J.; Kinberger, G. A.; Gaus, H. J.; Low, A.; Østergaard, M. E.; Bell, M.; Swayze, E. E.; Seth, P. P., Characterizing the effect of GalNAc and phosphorothioate backbone on binding of antisense oligonucleotides to the asialoglycoprotein receptor. *Nucleic Acids Res* **2017,** *45* (5), 2294-2306.
26. Medina, S. H.; Tekumalla, V.; Chevliakov, M. V.; Shewach, D. S.; Ensminger, W. D.; El-Sayed, M. E., N-acetylgalactosamine-functionalized dendrimers as hepatic

cancer cell-targeted carriers. *Biomaterials* **2011,** *32* (17), 4118-29.
27. Chen, S.; Tam, Y. Y.; Lin, P. J.; Leung, A. K.; Tam, Y. K.; Cullis, P. R., Development of lipid nanoparticle formulations of siRNA for hepatocyte gene silencing following subcutaneous administration. *J Control Release* **2014,** *196*, 106-12.
28. Tomiya, N.; Jardim, J. G.; Hou, J.; Pastrana-Mena, R.; Dinglasan, R. R.; Lee, Y. C., Liver-targeting of primaquine-(poly-γ-glutamic acid) and its degradation in rat hepatocytes. *Bioorg Med Chem* **2013,** *21* (17), 5275-81.
29. David, C.; Mengwen, Z.; Jason, R.; Jake, S.; Emily, B.; Egor, C.; Venkata, S.; Angela, G.; David, M.; Viswanathan, M.; David, S., Bifunctional Small Molecules That Mediate the Degradation of Extracellular Proteins. *ChemRxiv* **2020, July 29**.
30. Green, A.; Steven, B.; Caitlyn L., M.; Nicholas, R.; Jennifer R., C.; Carolyn, B., Lysosome Targeting Chimeras (LYTACs) That Engage a Liver-Specific Asialoglycoprotein Receptor for Targeted Protein Degradation. *ChemRxiv* **2020, July 30**.
31. Yang, K.; Song, Y.; Xie, H.; Wu, H.; Wu, Y. T.; Leisten, E. D.; Tang, W., Development of the first small molecule histone deacetylase 6 (HDAC6) degraders. *Bioorg Med Chem Lett* **2018,** *28* (14), 2493-2497.
32. Wang, B.; Wu, S.; Liu, J.; Yang, K.; Xie, H.; Tang, W., Development of selective small molecule MDM2 degraders based on nutlin. *Eur J Med Chem* **2019,** *176*, 476-491.
33. Roberts, B. L.; Ma, Z. X.; Gao, A.; Leisten, E. D.; Yin, D.; Xu, W.; Tang, W., Two-Stage Strategy for Development of Proteolysis Targeting Chimeras and its Application for Estrogen Receptor Degraders. *ACS Chem Biol* **2020,** *15* (6), 1487-1496.
34. Yang, K.; Zhao, Y.; Nie, X.; Wu, H.; Wang, B.; Almodovar-Rivera, C. M.; Xie, H.; Tang, W., A Cell-Based Target Engagement Assay for the Identification of Cereblon E3 Ubiquitin Ligase Ligands and Their Application in HDAC6 Degraders. *Cell Chem Biol* **2020,** *27* (7), 866-876.e8.
35. Wang, H. Y.; Blaszczyk, S. A.; Xiao, G.; Tang, W., Chiral reagents in glycosylation and modification of carbohydrates. *Chem Soc Rev* **2018,** *47* (3), 681-701.
36. Blaszczyk, S. A.; Homan, T. C.; Tang, W., Recent advances in site-selective functionalization of carbohydrates mediated by organocatalysts. *Carbohydr Res* **2019,** *471*, 64-77.
37. Douglass, E. F.; Miller, C. J.; Sparer, G.; Shapiro, H.; Spiegel, D. A., A comprehensive mathematical model for three-body binding equilibria. *J Am Chem Soc* **2013,** *135* (16), 6092-9.
38. Vincent, P.; Samuel, D., A comparison of the binding of biotin and biotinylated macromolecular ligands to an anti-biotin monoclonal antibody and to streptavidin. *J Immunol Methods* **1993,** *165* (2), 177-82.
39. Udeshi, N. D.; Pedram, K.; Svinkina, T.; Fereshetian, S.; Myers, S. A.; Aygun, O.; Krug, K.; Clauser, K.; Ryan, D.; Ast, T.; Mootha, V. K.; Ting, A. Y.; Carr, S. A., Antibodies to biotin enable large-scale detection of biotinylation sites on proteins. *Nat Methods* **2017,** *14* (12), 1167-1170.

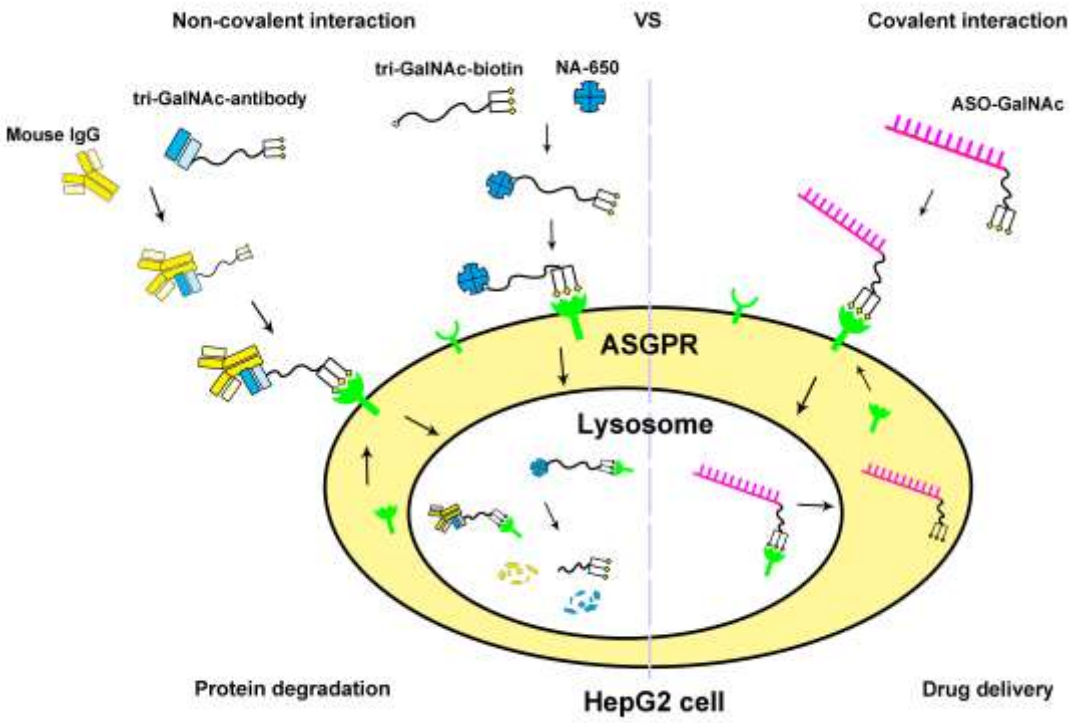

Figure. 1. Comparison of the application of tri-GalNAc in targeted protein degradation and drug delivery. Small molecule- and antibody-based tri-GalNAc degraders non-covalently capture the protein targets and transport the targets to lysosome for degradation via the interaction with ASGPR. Oligonucleotides covalently linked to tri-GalNAc enable their internalization into the cell through ASGPR. After trafficking to lysosome, small amount of the oligonucleotides can escape from the endosome or lysosome to block or induce degradation of RNA.

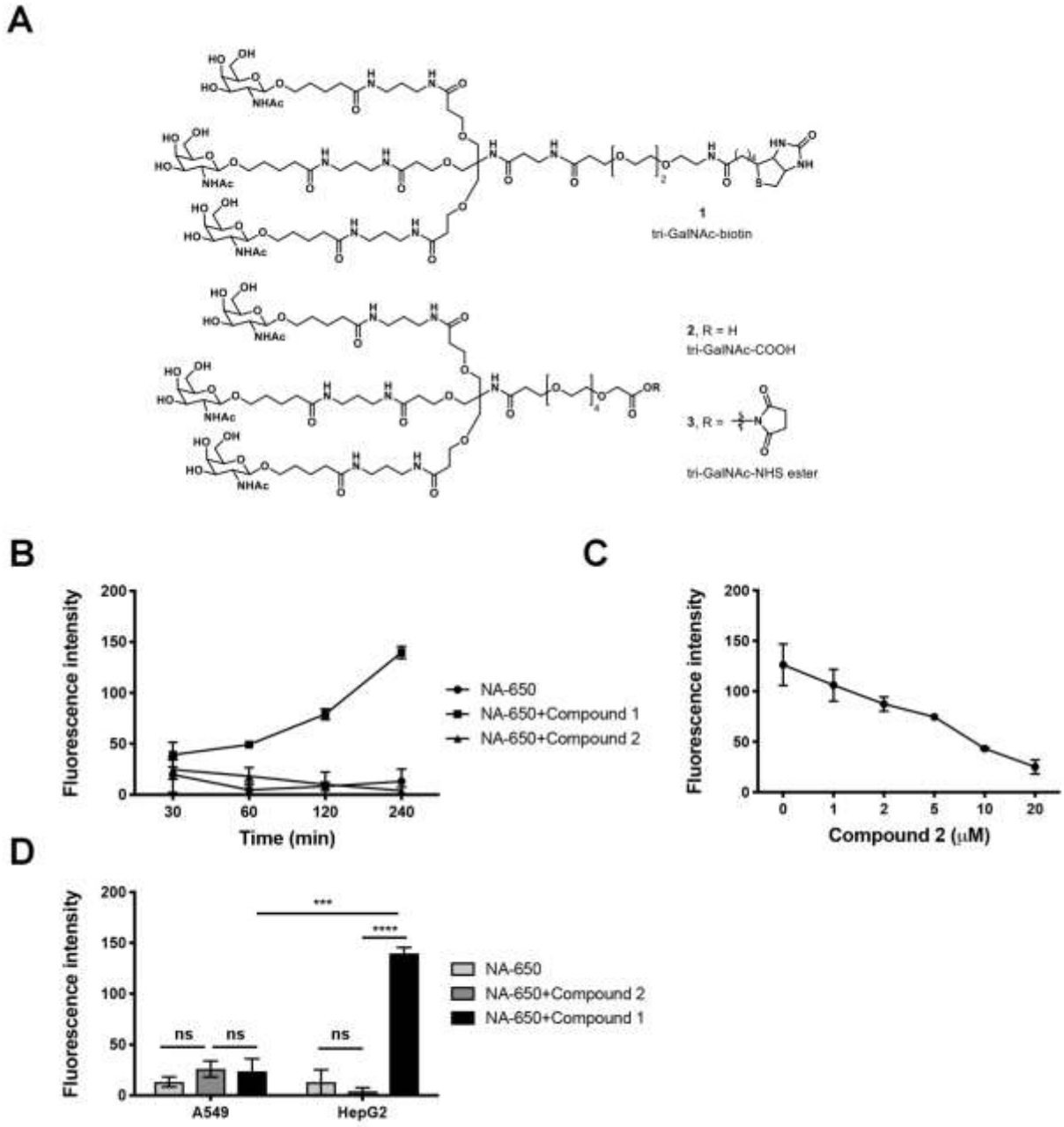

Figure. 2. Tri-GalNAc-biotin mediates ASGPR-dependent cellular uptake of NA-650 specifically in HepG2 Cells. A. Chemical structures of tri-GalNAc-biotin (compound **1**), tri-GalNAc-COOH (compound **2**), and tri-GalNAc-NHS ester (compound **3**). **B.** Cellular uptake of NA-650 in HepG2 cells treated with NA-650 alone (500 nM) or NA-650 (500 nM) and compound **1** (2 μM) or **2** (2 μM). **C.** Inhibition of the internalization of NA-650 (500 nM) mediated by **1** (2 μM) in HepG2 cells by compound **2**. **D.** Comparison of the internalization of NA-650 (500 nM) mediated by **1** (2 μM) between A549 cells and HepG2 cells incubated with NA-650 alone or NA-650 and Compound **1** or **2**. Data presented as Mean±SD, n=3. Ns: not significant, ***p<0.001, ****p<0.0001.

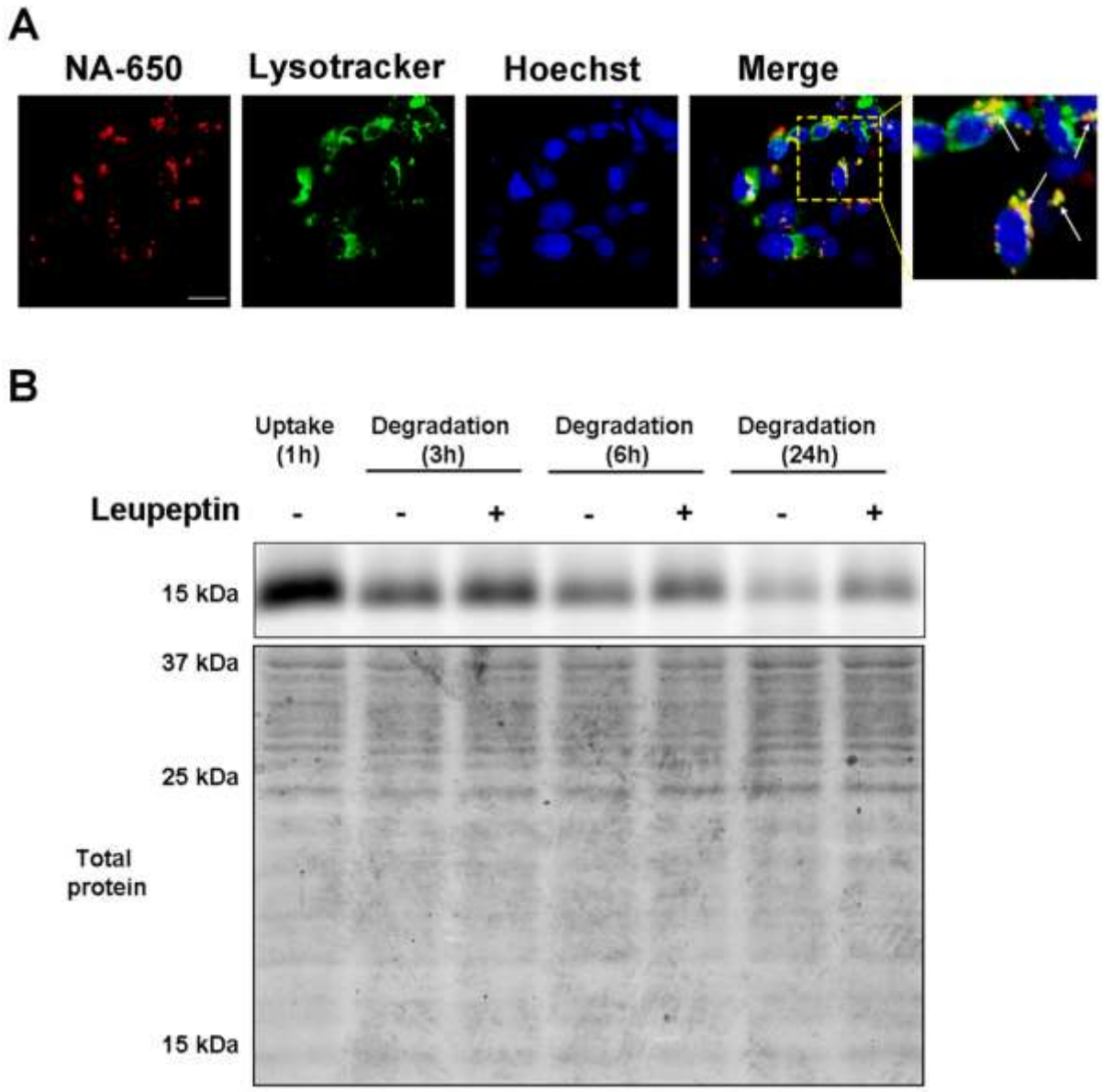

Figure. 3. Tri-GalNAc-biotin 1 transports NA-650 to lysosome for degradation. A. Confocal microscopy images of HepG2 cells treated with NA-650 (500 nM) and compound **1** (2 μM) for 18 h. Red: internalized NA-650; Green: lysosome stained by Lysotracker; Blue: nuclei stained by Hoechst 33342; Yellow: merged area. White arrows indicate the co-localization of NA-650 and the lysosome. Scale bar: 20 μm. **B.** In gel fluorescence analysis of NA-650 (500 nM) internalization and degradation in HepG2 cells by compound **1** (2 μM) in the presence or absence of leupeptin (0.1 mg/mL).

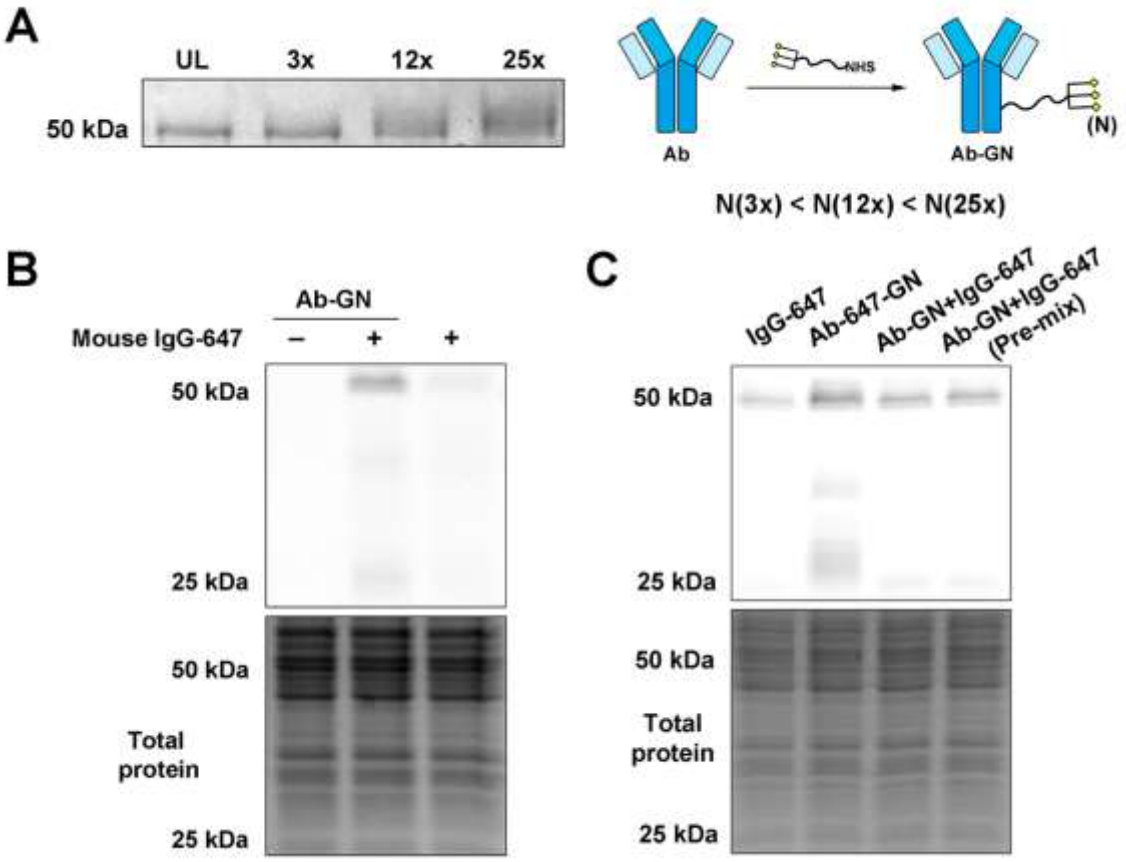

Figure. 4. A tri-GalNAc labelled full length antibody goat anti-mouse IgG (Ab-GN) inefficiently delivers target protein mouse anti-biotin IgG-647 into the cells. A. Goat anti-mouse full length antibody labeling with various amounts of tri-GalNAc. UL: unlabeled; 3x: 3 molar equivalent; 12x: 12 molar equivalent; 25x: 25 molar equivalent. N: the number of tri-GalNAc labeled on the antibody. **B.** Uptake of mouse anti-biotin IgG-647 (50 nM) in the HepG2 cells treated with or without Ab-GN (25 nM) for 6 h. **C.** Mouse anti-biotin IgG-647 (50 nM) uptake mediated by Ab-GN (25 nM) with or without 1 h pre-mix before treatment for 6 h. The uptake of anti-biotin IgG-647 (50 nM) and Ab-647-GN (25 nM) were measured for comparison.

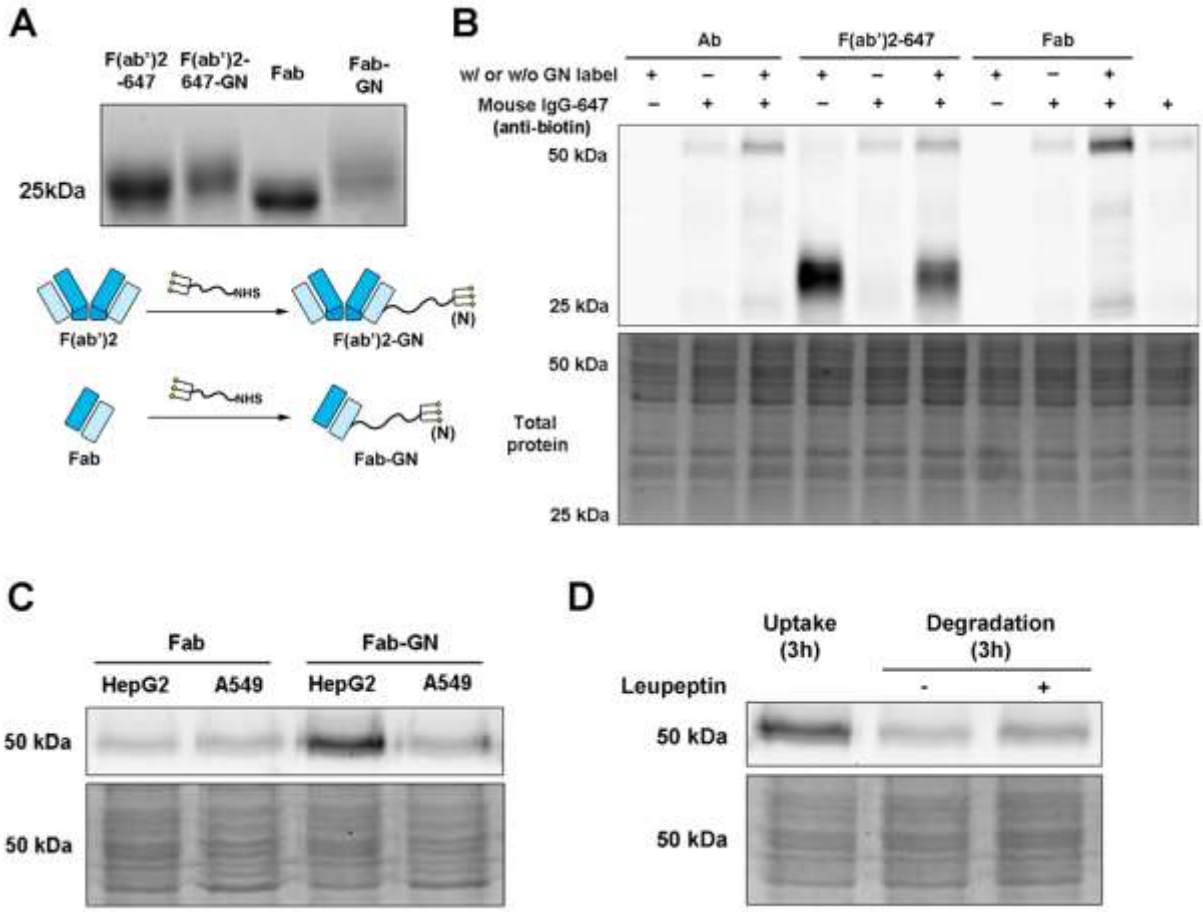

Figure. 5. Tri-GalNAc labeled antibody fragments enhance the endocytosis of mouse anti-biotin IgG-647 and degrade the target protein in lysosome. A. Antibody fragments labeling with tri-GalNAc (25 molar equivalent). **B.** Comparison of the 6 h uptake of mouse anti-biotin IgG-647 (50 nM) mediated by 25 nM of the goat anti-mouse IgG, goat anti-mouse IgG F(ab')2-647 and goat anti-mouse IgG Fab with or without tri-GalNAc (GN) labeling (3rd and 2nd column of each of the three groups, respectively). Cells treated with mouse anti-biotin IgG-647 alone (last column) or Ab-GN, F(ab')2-GN and Fab-GN alone (1st column of each of three groups) were used as control groups. **C.** Internalization of mouse anti-biotin IgG-647 in A549 cells and HepG2 cells incubated with mouse anti-biotin IgG-647 (50 nM) and 25 nM of goat anti-mouse IgG Fab with or without tri-GalNAc (GN) labeling for 6 h. **D.** Mouse anti-biotin IgG-647 (50 nM) endocytosis and degradation in HepG2 cells in the presence or absence of leupeptin (0.1 mg/mL) for 6 h.

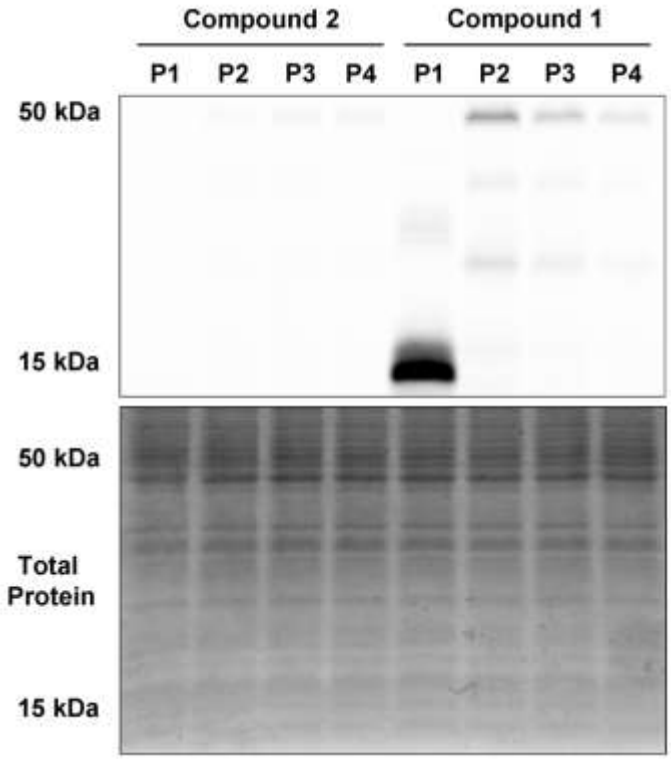

Figure. 6. Tri-GalNAc-biotin 1 triggers more internalization of target proteins with smaller size. Cellular uptake of NA-650 (P1, 50 nM), mouse anti-biotin IgG-647 (P2, 50 nM), pre-mixed mouse anti-biotin IgG-647 (50 nM) / goat anti-mouse IgG Fab (200 nM) complex (P3) and pre-mixed mouse anti-biotin IgG-647 (50 nM) / goat anti-mouse IgG (200 nM) complex (P4) in the presence of compound **1** (200 nM) or **2** (200 nM) for 6 h.

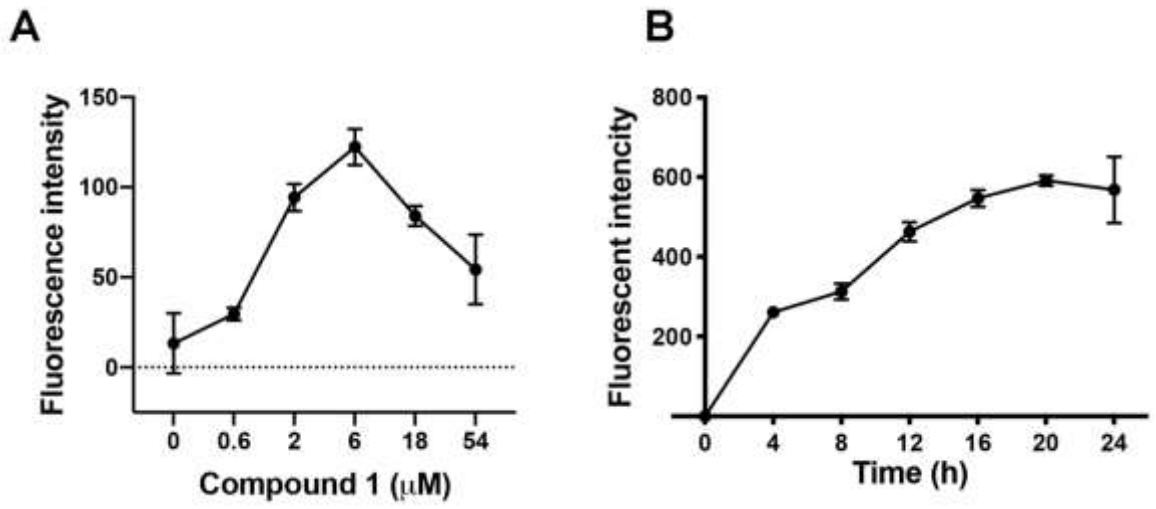

Figure. S1. Tri-GalNAc-biotin mediates the uptake of NA-650 in a time- and dose-dependent manner. A. NA-650 uptake in HepG2 cells treated with NA-650 (500 nM) and increasing concentrations of compound **1** for 4 h. **B.** Cellular uptake of NA-650 (500 nM) in HepG2 cells in the presence of compound **1** (2 μM) within 24 h.

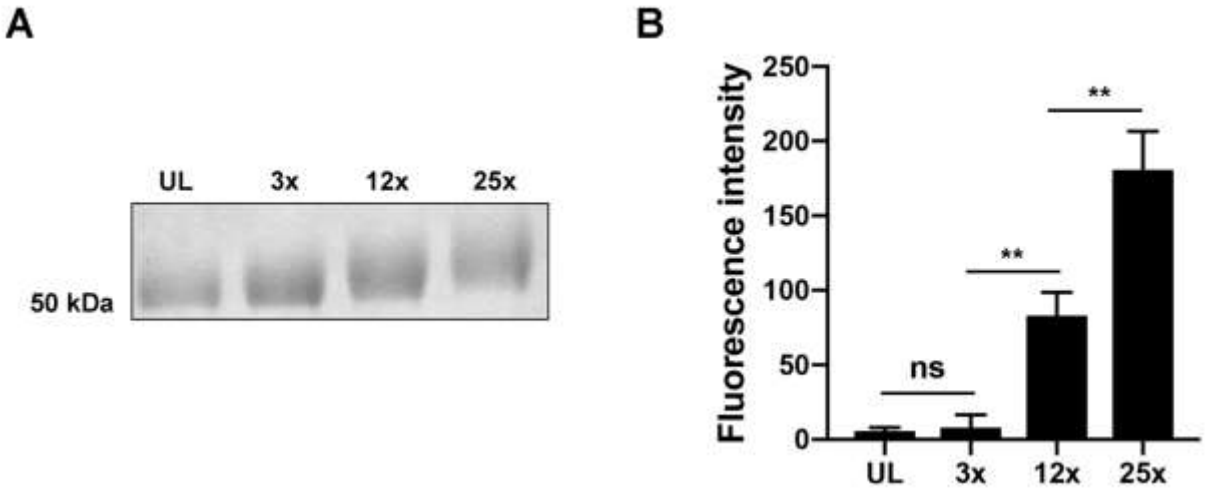

Figure. S2. Tri-GalNAc-Antibody (Ab-647-GN) with higher degree of modification exhibits greater uptake efficiency. A. Goat anti-mouse-647 antibody labeled with various amounts of tri-GalNAc. UL: unlabeled; 3x: 3 molar equivalent; 12x: 12 molar equivalent; 25x: 25 molar equivalent. **B.** Cellular uptake of Ab-647-GN (25 nM) with different degrees of labeling in 16 h. Data presented as Mean±SD, n=3. Ns: not significant, **p<0.01.

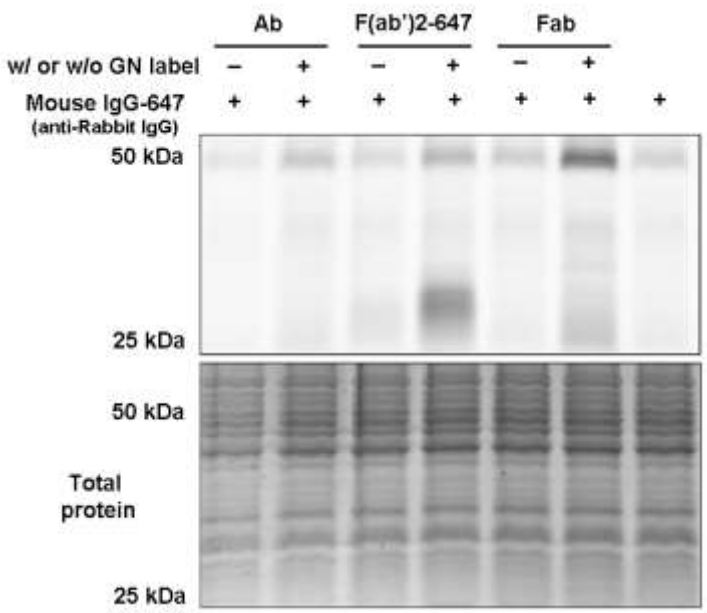

Figure. S3. Tri-GalNAc labeled antibody Fab fragment mediates the highest endocytosis of mouse anti-rabbit IgG-647. HepG2 cells were treated with mouse anti-rabbit IgG-647 (50 nM) in the presence of 25 nM of goat anti-mouse IgG, goat anti-mouse IgG F(ab')2-647 and goat anti-mouse IgG Fab with or without tri-GalNAc labeling. Cells with only mouse anti-rabbit IgG-647 (last column) were set as the control. The uptake was measured and compared after 6 h treatment.